

# $\Sigma^-$ atoms and the $\Sigma N$ interaction

J. Dąbrowski<sup>1,a</sup>, J. Rożynek<sup>1</sup>, and G.S. Anagnostatos<sup>2</sup>

<sup>1</sup> Theoretical Division, Sołtan Institute for Nuclear Studies, Hoza 69, Pl-00-681 Warsaw, Poland

<sup>2</sup> Institute of Nuclear Physics, National Center for Scientific Research “Democritos”, GR-153-10 Aghia Paraskevi. Attiki, Greece

Received: 15 January 2002 / Revised version: 7 March 2002  
Communicated by M. Garçon

**Abstract.** It is shown that among four models of the Nijmegen baryon-baryon interaction only model F—which leads to a repulsive potential felt by the  $\Sigma$  hyperon inside the nucleus—is consistent both with the analysis of  $\Sigma^-$  atoms and of the  $(K^-, \pi)$  reactions. The Nijmegen models are used to determine the strong complex single-particle (s.p.) potential of  $\Sigma^-$ , and to calculate the strong-interaction shifts and widths of the lowest observed levels of  $\Sigma^-$  atoms. The results obtained with model F are in best agreement with the experimental data.

**PACS.** 13.75.Ev Hyperon-nucleon interactions – 36.10.Gv Mesonic atoms and molecules, hyperonic atoms and molecules

## 1 Introduction

Observed properties of  $\Sigma^-$  atoms, *i.e.*, strong-interaction shifts  $\epsilon$  and widths  $\Gamma$  of the lowest observed levels, provide us with valuable information on the strong interaction between  $\Sigma^-$  and the nucleons, as well as on the nucleon density distribution in the nucleus of the  $\Sigma^-$  atom. In a recent comprehensive phenomenological analysis of the existing  $\Sigma^-$  data Batty, Friedman, and Gal [1] found the following striking property of the single-particle (s.p.) strong-interaction potential of  $\Sigma^-$ : it is repulsive inside the nucleus and attractive outside. The need for the repulsion arose when new data were included into the analysis, namely the results of Powers *et al.* [2], especially their precise data on the  $\Sigma^-$ Pb atom.

This behavior of  $\Sigma^-$  s.p. potential found in the analysis of  $\Sigma^-$  atoms is consistent with the analysis of the pion spectra measured in  $(K^-, \pi)$  reactions, which suggests a  $\Sigma$  s.p. potential repulsive inside nuclei [3, 4] (with a substantial positive Lane potential  $V_\tau$  [5]). This repulsion follows directly from the observed shift of the pion spectra toward higher  $\Sigma$  energies compared to the quasi-free spectrum.

The discussion in [3, 4] concerns the recent Brookhaven  $(K^-, \pi)$  experiments on  $^9\text{Be}$  target [6], which were performed with an order-of-magnitude better statistics than the earlier CERN experiments [7]. Because of poor accuracy of the pion spectra measured in the early experiments, we did not use these spectra in our analysis of the  $\Sigma N$  interaction. Nevertheless, it remains a valid observation that no  $\Sigma$  bound states were detected in the old CERN as well as in the new Brookhaven experiments

(except for the bound state of  $^4_\Sigma\text{He}$ ). This fact is a clear indication that the s.p.  $\Sigma$  potential inside nuclei is repulsive<sup>1</sup>.

Thus the analysis of both  $\Sigma^-$  atoms and the  $(K^-, \pi)$  reactions leads to the conclusion that the  $\Sigma$  s.p. potential is repulsive inside the nucleus. Obviously, just outside the nuclear core, it is attractive, since the strong interaction increases the binding of the  $\Sigma^-$  atomic states. These desired properties of the  $\Sigma$  s.p. potential should follow from a realistic  $\Sigma N$  interaction<sup>2</sup>. It is our purpose to calculate the  $\Sigma$  s.p. potential for a variety of  $\Sigma N$  interactions and in this way to find out which of them is most realistic.

In the present paper we consider the Nijmegen models of the baryon-baryon interaction: models D [11], F [12], soft-core (SC) model [13], and the new soft-core (NSC) model [14]. In our analysis, we apply the effective  $\Sigma^- N$  interaction in nuclear matter,  $\mathcal{K}$ , obtained within the low-order Brueckner (LOB) theory with the above interaction models by Yamamoto, Motoba, Himeno, Ikeda, and Nagata [15], and by Rijken, Stoks, and Yamamoto [14] (the so-called YNG interactions).

The single-particle (s.p.) potential  $V$  of the  $\Sigma^-$  moving with momentum  $\hbar k_\Sigma$  in nuclear matter with nucleon density  $\rho$  and neutron excess  $\alpha = (N - Z)/A$  has the

<sup>1</sup> Notice also that a theoretical description of the only  $\Sigma$  bound state observed in the Brookhaven experiments [8] on  $^4\text{He}$  target was achieved by Harada [9] with the help of the phenomenological  $\Sigma N$  interaction leading to the  $\Sigma$  s.p. potential which is repulsive inside the nuclear core and has an attractive tail.

<sup>2</sup> Within the relativistic mean-field approach, these properties of  $V$  have been discussed in [10].

<sup>a</sup> e-mail: dabrnucl@fuw.edu.pl

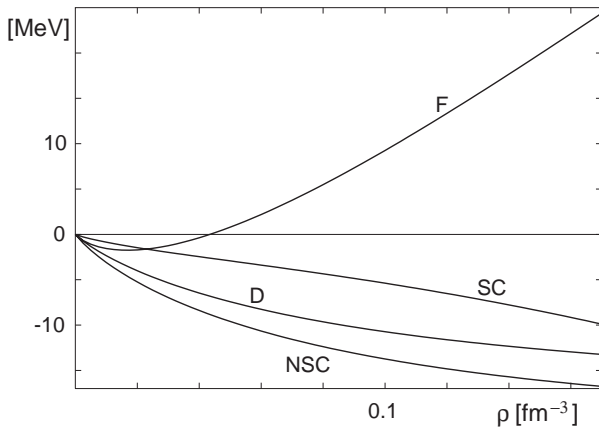


**Fig. 1.** The isoscalar  $\Sigma$  potential in nuclear matter  $V_0$  as a function of the nucleon density  $\rho$  for  $k_\Sigma = 0$ .

form [5]:

$$V_{\text{NM}}(k_\Sigma, \rho, \alpha) = V_0(k_\Sigma, \rho) + \frac{1}{2}\alpha V_\tau(k_\Sigma, \rho). \quad (1)$$

Here, we ignore terms connected with spin excess, considered in [16], which are usually negligibly small.

Expressions for the isoscalar potential  $V_0$  and for the Lane potential  $V_\tau$  in terms of the effective  $\Sigma N$  interaction  $\mathcal{K}$  are given in [5]. When we apply the expression for  $V_0$  to the YNG effective  $\Sigma N$  interactions, we get the results shown in fig. 1<sup>3</sup>. (Because of the relatively small magnitude of  $\Sigma$  momenta in  $\Sigma^-$  atoms, the value  $k_\Sigma = 0$  is used in fig. 1.) We see that only the model F of the Nijmegen baryon-baryon interaction leads to repulsive  $V_0$  at nucleon densities  $\rho \gtrsim 0.05 \text{ fm}^{-3}$  encountered inside nuclei, and to attractive  $V_0$  at lower densities encountered in the nuclear surface. All the remaining models lead to attractive  $V_0$  at all densities. This means that only the model F leads to the  $\Sigma$  s.p. potential which is in qualitative agreement with the phenomenological analysis [1] of  $\Sigma^-$  atoms<sup>4</sup> and also with the pion spectra measured in the  $(K^-, \pi)$  reactions.

The important question is whether the model F can explain quantitatively the measured properties of the  $\Sigma^-$  atoms. It is the purpose of the present paper to show that this is indeed the case. Using model F, we calculate the energy shifts  $\epsilon$  and widths  $\Gamma$  of the  $\Sigma^-$  atomic levels, and show that they are reasonably close to experimental data.

The YNG  $\Sigma N$  interaction was applied before in the theory of  $\Sigma^-$  atoms by Yamada and Yamamoto [17] in an attempt to explain the early  $\Sigma^-$  atomic data. These authors calculated the energy shift  $\epsilon$  and the width  $\Gamma$  of the lowest state in  $^{16}\text{O}$ ,  $^{24}\text{Mg}$ ,  $^{28}\text{Si}$  and  $^{32}\text{S}$   $\Sigma^-$  atoms. They used the Hartree-Fock nuclear wave functions calculated with the Skyrme interaction. Their F model results for both  $\epsilon$  and  $\Gamma$  are much bigger than our results, and

<sup>3</sup> Here we consider the real s.p. potential  $V$  and use the real part of the YNG interactions.

<sup>4</sup> The behavior of  $V_\tau$  is irrelevant here, because the analysis in [1] was applied also to the  $\Sigma^-$  atoms with  $N = Z$  in which  $V_\tau$  plays a negligible role.

clearly disagree with the experimental data. The reason might be the nuclear wave functions used in [17] which do not reproduce the empirical charge distribution.

The paper is organized as follows. Our theoretical scheme is presented in sect. 2. In sect. 2.1 the expression for the real s.p. potential of  $\Sigma^-$ ,  $V$ , is derived. In sect. 2.2, we derive our expression for the  $\Sigma^-$  absorptive s.p. potential  $W$ . Our choice of the proton and the neutron densities is discussed in sect. 2.3. Our results for the energy shifts and widths are presented, compared with experiment, and discussed in sect. 3. The energy conservation and the action of the exclusion principle in the  $\Sigma A$  conversion process in nuclear matter is outlined in the appendix.

## 2 The theoretical scheme

To determine  $\epsilon$  and  $\Gamma$ , we solve the Schrödinger equation, which describes the motion of  $\Sigma^-$  in the  $\Sigma^-$  atom:

$$[-(\hbar^2/2\mu_{\Sigma A})\Delta + V_C(r) + \mathcal{V}(r)]\Psi = \mathcal{E}\Psi, \quad (2)$$

where  $\mu_{\Sigma A} = M_\Sigma M_A / (M_\Sigma + M_A)$  is the  $\Sigma^-$ -nucleus (of mass  $M_A$ ) reduced mass ( $M_\Sigma$  is the mass of  $\Sigma^-$ ), and  $V_C$  is the Coulomb interaction between  $\Sigma^-$  and the nucleus.

Because of the  $\Sigma A$  conversion process  $\Sigma^- p \rightarrow \Lambda n$ , the strong-interaction potential  $\mathcal{V}$  is complex,  $\mathcal{V} = V + iW$ , and consequently the eigenvalue  $\mathcal{E}$  is also complex, with its imaginary part connected with the width of the level,  $\mathcal{E} = E - i\Gamma/2$ . For the strong-interaction energy shift  $\epsilon$ , we have  $\epsilon = E_C - E$ , where  $E_C$  is the pure Coulomb energy, *i.e.*, the eigenvalue of eq. (2) without the strong-interaction potential  $\mathcal{V}$ . Notice that  $\epsilon$  is positive for downward shift of the level. The measured energy of  $\gamma$  transition to the level is then increased by  $\epsilon^5$ .

To calculate the real and absorptive strong-interaction potentials  $V$  and  $W$ , we apply the local density approximation (LDA): the  $\Sigma^-$  atom is treated at each point as  $\Sigma^-$  moving in nuclear matter with the local nuclear density of the  $\Sigma^-$  atom.

### 2.1 Expression for V

Let us consider a  $\Sigma^-$  atom with proton and neutron density distributions  $\rho_p(r)$  and  $\rho_n(r)$ , respectively. At any distance  $r$ , we treat the system as nuclear matter with total nucleon density  $\rho(r) = \rho_p(r) + \rho_n(r)$  and with neutron excess  $\alpha(r) = [\rho_n(r) - \rho_p(r)]/\rho(r)$ , and with a  $\Sigma^-$  hyperon with momentum  $k_\Sigma \approx 0$ . (The last approximation is justified by the very weak dependence of the  $\Sigma$  s.p. potential in nuclear matter on  $k_\Sigma$  found in [5], and by the relatively small magnitude of  $\Sigma$  momenta in  $\Sigma^-$  atoms

<sup>5</sup> Strictly speaking, the energy of  $\gamma$  transition is increased by  $\epsilon - \epsilon^u$ , where  $\epsilon^u$  is the energy shift of the upper, initial state of the transition. In general, however,  $\epsilon^u$  is negligible small compared to  $\epsilon$ , except maybe in the case of Pb in which we expect  $\epsilon^u \simeq 20 \text{ eV}$ .

(see values of  $\bar{k}_\Sigma$  presented in sect. 3.) To get the value of the  $\Sigma^-$  s.p. potential in  $\Sigma^-$  atom at a distance  $r$ , we calculate  $V_{0,\tau}(k_\Sigma, \rho(r))$  at  $k_\Sigma = 0$  by applying the expressions given in [5] with the YNG effective interactions of [15] (and [14]). In this way we obtain the isoscalar and the Lane potentials in  $\Sigma^-$  atom at a distance  $r$ ,

$$V_0(r) = V_0(k_\Sigma=0, \rho(r)), \quad V_\tau(r) = V_\tau(k_\Sigma=0, \rho(r)), \quad (3)$$

and the total nuclear s.p.  $\Sigma^-$  potential,

$$V(r) = V_0(r) + \frac{1}{2}\alpha(r)V_\tau(r). \quad (4)$$

## 2.2 Expression for $W$

Here we follow the procedure applied in [18] in explaining the early data on  $\Sigma^-$  atomic widths. A slightly simplified form of our expression (5) for  $W_{\text{NM}}$  in terms of the  $\Sigma A$  conversion cross-section was used before in [19]. In the context of  $\Sigma$  nuclear interaction a semiclassical expression for  $W$  in terms of the  $\Sigma A$  conversion cross-section was first discussed by Gal and Dover [20].

First, let us consider a  $\Sigma^-$  hyperon moving with momentum  $\hbar k_\Sigma$  in nuclear matter with total and proton densities  $\rho$ ,  $\rho_p$ . The width  $\Gamma_{\text{NM}}$  of this state is connected with the absorptive potential  $W_{\text{NM}} = -\frac{1}{2}\Gamma_{\text{NM}}$ . By applying the optical theorem to the Brueckner reaction matrix  $\mathcal{K}$  —as was shown in [19] and [18]— one obtains for  $W_{\text{NM}}$

$$W_{\text{NM}}(k_\Sigma, \rho, \rho_p) = -\frac{1}{2}\nu'\rho_p \frac{\hbar^2}{\mu_{\Sigma N}} \langle k_{\Sigma N} Q \sigma \rangle, \quad (5)$$

where  $\langle \rangle$  denotes the average value in the Fermi sea,  $\hbar k_{\Sigma N}$  is the  $\Sigma^- N$  relative momentum,  $\mu_{\Sigma N}$  is the  $\Sigma^- N$  reduced mass,  $\nu'$  is the ratio of the effective to the real nucleon mass,  $Q$  is the exclusion principle operator (see appendix for details), and  $\sigma$  is the total cross-section for the  $\Sigma A$  conversion process.

Strictly speaking, the optical theorem leads to expression (5) in which not  $\sigma$  but  $\sigma_{\text{NM}}$ , the  $\Sigma A$  conversion cross-section in nuclear matter, appears. It is expressed by the  $\mathcal{K}$  matrix in the same way as the free scattering cross-section is expressed by the scattering matrix. As was discussed in [19] and [18], the approximation  $\sigma_{\text{NM}} \simeq \sigma$  works very well even at equilibrium density of nuclear matter, and becomes excellent at low densities relevant for  $\Sigma^-$  atoms because the Brueckner  $\mathcal{K}$  matrix with decreasing density approaches the free scattering matrix.

With the absorptive potential  $W(r)$  in a  $\Sigma^-$  atom with total and proton densities  $\rho(r)$ ,  $\rho_p(r)$ , we proceed similarly as with  $V$  and write

$$W(r) = W_{\text{NM}}(\bar{k}_\Sigma, \rho(r), \rho_p(r)). \quad (6)$$

Here, we insert for  $k_\Sigma$  in (5) the average momentum of  $\Sigma^-$  in the rest frame of the nuclear medium,  $\bar{k}_\Sigma$ , connected with the average relative  $\Sigma^-$ -nucleus momentum  $k_{\Sigma A}$  by:  $\bar{k}_\Sigma = M_\Sigma \bar{k}_{\Sigma A} / \mu_{\Sigma A}$ . We determine  $\bar{k}_{\Sigma A}$  from

$$\hbar^2 \bar{k}_{\Sigma A}^2 / 2\mu_{\Sigma A} = \langle \psi | T | \psi \rangle = Z e^2 / 2a_n, \quad (7)$$

where in the last step we calculated  $\langle \psi | T | \psi \rangle$ , the average kinetic energy of the relative  $\Sigma^-$ -nucleus motion, with the help of the hydrogen-like function  $\psi$  of the orbit with principal quantum number  $n$  ( $a_n = (n^2 / Z e^2) \hbar^2 / \mu_{\Sigma A}$  is the radius of the orbit).

For the total  $\Sigma A$  conversion cross-section  $\sigma$  we shall use the parametrization, adjusted by Gal, Tokar, and Alexander [21] to the  $\Sigma^-$  low-energy regime up to 300 MeV/c in the laboratory frame. It has the form

$$(v/c)\sigma = (1 + 13v/c)^{-1} 5.1 \text{ fm}^2, \quad (8)$$

where  $v$  is the relative velocity of  $\Sigma^-$  and proton. Expression (8) gives for  $(v/c)\sigma$  results very close to the results obtained with model F (see [12]). Consequently, using expression (5) with  $v\sigma$  given by expression (8) is equivalent to (and much simpler than) calculating  $W_{\text{MN}}$  starting with model F of the hyperon-nucleon interaction. Notice that at very small nucleon densities, relevant in  $\Sigma^-$  atoms, the  $\mathcal{K}$  matrix is identical with the free scattering matrix whose imaginary part —via the optical theorem— is proportional to  $v\sigma$ .

## 2.3 Proton and neutron density distributions

The proton and neutron density distributions,  $\rho_p(r)$  and  $\rho_n(r)$  used in our calculation have been obtained from the isomorphic shell model (ISM).

The ISM model differs from the conventional shell model by the state dependence of the s.p. Hamiltonian: the s.p. potential is different in each shell —in each of them it is assumed to have the shape of a harmonic oscillator [22]. The way of determining the parameters of these harmonic-oscillator potentials is explained in [23] (see also [24] and references therein). The important point is that the ISM model reproduces reasonably well the total nuclear binding, and —what is particularly important in our calculations— the proton and neutron separation energies and the empirical charge distributions.

The final version of the ISM neutron densities in the case of  $^{184}\text{W}$  and  $^{208}\text{Pb}$  are not available, and in these two cases we assumed that the neutron density has the same shape as the proton density, *i.e.*, we put  $\rho_n(r) = (N/Z)\rho_p(r)$ . We checked that this procedure when applied in cases of all other nuclei considered here would have only a very small effect on the calculated values of  $\epsilon$ .

## 3 Results and discussion

For the the Coulomb interaction  $V_C$  in Schrödinger equation (2), we use the potential produced by a uniform charge distribution with radius  $R$ , which leads to the same r.m.s. radius  $\langle r^2 \rangle^{1/2}$  of the charge distribution,  $R = \sqrt{3/5} \langle r^2 \rangle^{1/2}$ . For the r.m.s. radii, we use the empirical values collected in [25]. They are listed in [26] together with the predictions of the ISM model, which are in good agreement with each other. If we used these predictions instead

**Table 1.** Energy shifts  $\epsilon$ ,  $\epsilon^u$  and widths  $\Gamma$ ,  $\Gamma^u$  calculated with model F of the  $\Sigma N$  interaction, respectively for the lower and upper level of the indicated  $\Sigma^-$  atoms together with the experimental results. All energies are in eV.

Nucleus	$n + 1 \rightarrow n$	$\epsilon$	$\epsilon_{\text{exp}}$	$\Gamma$	$\Gamma_{\text{exp}}$	$\epsilon^u$	$\Gamma^u$	$\Gamma_{\text{exp}}^u$
$^{12}\text{C}$	$4 \rightarrow 3$	8.19	–	22.2	–	0.007	0.011	$0.031 \pm 0.012^a$
$^{16}\text{O}$	$4 \rightarrow 3$	50.0	$320 \pm 230^b$	194.2	–	0.11	0.20	$1.0 \pm 0.7^b$
$^{24}\text{Mg}$	$5 \rightarrow 4$	32.6	$25 \pm 40^b$	50.4	$< 70^b$	0.08	0.10	$0.11 \pm 0.09^b$
$^{27}\text{Al}$	$5 \rightarrow 4$	67.3	$68 \pm 28^b$	113.2	$43 \pm 75^b$	0.22	0.28	$0.24 \pm 0.06^b$
$^{28}\text{Si}$	$5 \rightarrow 4$	139.9	$159 \pm 36^b$	242.8	$220 \pm 110^b$	0.55	0.70	$0.41 \pm 0.10^b$
$^{32}\text{S}$	$5 \rightarrow 4$	433.8	$360 \pm 220^b$	873.2	$870 \pm 700^b$	2.49	3.43	$1.5 \pm 0.8^b$
$^{40}\text{Ca}$	$6 \rightarrow 5$	27.0	–	42.0	–	0.12	0.15	$0.41 \pm 0.22^a$
$^{48}\text{Ti}$	$6 \rightarrow 5$	44.9	–	104.0	–	0.30	0.48	$0.65 \pm 0.42^a$
$^{138}\text{Ba}$	$9 \rightarrow 8$	32.6	–	73.9	–	0.92	1.34	$2.9 \pm 3.5^a$
$^{184}\text{W}$	$10 \rightarrow 9$	126.7	$214 \pm 60^c$	180.5	$18 \pm 149^c$	3.75	4.24	$2 \pm 2^c$
$^{208}\text{Pb}$	$10 \rightarrow 9$	457.4	$422 \pm 56^c$	773.4	$428 \pm 158^c$	18.9	23.8	$17 \pm 3^c$

<sup>a</sup> Data taken from ref. [27].

<sup>b</sup> Data taken from ref. [28].

<sup>c</sup> Data taken from ref. [2].

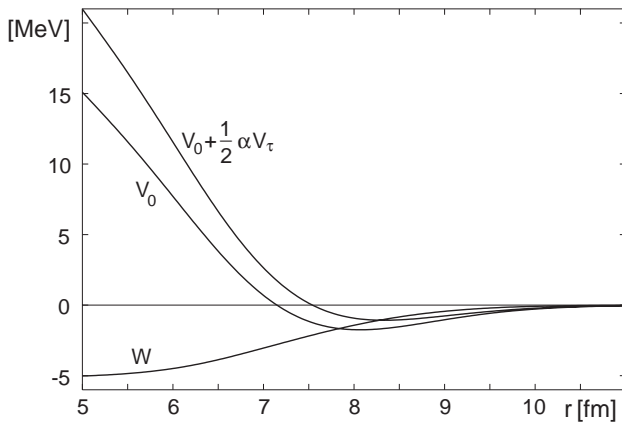


**Fig. 2.** Potentials  $V$  and  $W$  in  $^{208}\text{Pb}$ .

of the empirical values, our results would practically not change.

Our results for  $\epsilon$  and  $\Gamma$  are presented in table 1 together with the existing experimental data which, however, are relatively inaccurate. Our results appear reasonably close to the experimental data and indicate the consistency of model F with the properties of the  $\Sigma^-$  atoms. This leads us to the conclusion that among the Nijmegen baryon-baryon interactions, only model F —*i.e.*, the model which leads to the repulsive s.p. potential of  $\Sigma^-$  inside the nucleus— is capable to represent the  $\Sigma N$  interaction both in  $\Sigma$  hypernuclear states and in  $\Sigma^-$  atoms.

Our present results turn out to be very close to our previous simple estimates of  $\epsilon$  and  $\Gamma$ , obtained in [29] by applying the first-order perturbation approximation.

Let us make one remark more in favor of model F of the baryon-baryon interaction: when applied to the  $\Lambda$  + nuclear matter system it leads to the semiempirical value of the  $\Lambda$  binding energy, *i.e.*, it solves the so-called  $\Lambda$  overbinding problem [30].

In fig. 2 we show in the case of Pb the real and absorptive potentials  $V$  and  $W$ . Here,  $W$  has been calcu-

lated with  $\bar{k}_\Sigma = 0.40 \text{ fm}^{-1}$ , the average  $\Sigma^-$  momentum in the lower ( $n = 9$ ) state (if we used the average momentum in the upper ( $n = 10$ ) state, the resulting curve could hardly be distinguished from the  $W$  curve in fig. 2). There is a considerable difference between the  $V = V_0 + \frac{1}{2}\alpha V_\tau$  and  $V_0$  curves indicating the importance of the Lane potential  $V_\tau$ . If we neglected the Lane potential  $V_\tau$  in this case of the  $n = 9$  state in Pb we would get the result  $\epsilon[V_\tau = 0] = 713.5 \text{ eV}$  which is much bigger than the result  $457.4 \text{ eV}$  obtained with the full potential  $V = V_0 + \frac{1}{2}\alpha V_\tau$  and the experimental result  $422 \pm 56 \text{ eV}$ . This demonstrates that a substantial Lane potential is essential in the description of  $\Sigma^-$  atoms.

Let us consider the problem of the accuracy of our method of determining the  $\Sigma$  s.p. potential. We use the real potential  $V$  in nuclear matter, which was obtained in [15] and [14] by applying the LOB approximation which depends on the energy spectrum of the intermediate states used in the reaction matrix equation. Fortunately, most important in  $\Sigma^-$  atoms is  $V$  at nuclear surface and beyond, where the nuclear density is small and where consequently the choice of the energy spectrum in the reaction matrix equation is less important.

In calculating the  $\Sigma$  s.p. potential, we have applied the LDA. This approximation is expected to be reasonably accurate in regions where the nuclear density is varying slowly. This appears to be the situation in  $\Sigma^-$  atoms. Here, the strong interaction of  $\Sigma^-$  occurs predominantly in the tail of the nuclear density distribution where the derivative of the density tends to zero. For instance in the case of the lower  $n = 9$  level in the  $\Sigma^- \text{Pb}$  atom, the dominant contribution to  $\langle \Psi | V_\Sigma | \Psi \rangle$  comes from the region around  $r \sim 9 \text{ fm}$ , whereas  $\langle r^2 \rangle_{\text{Pb}}^{1/2} \simeq 5.5 \text{ fm}$ .

The accuracy of the LDA may be approximately estimated with the help of the improved LDA suggested in the case of the nucleon s.p. potential a long time ago by Jeukenne, Lejeune, and Mahaux [31]. If the density-dependent effective two-body interaction had zero range then the LDA would be exact. According to the improved

LDA the effect of the finite range of the  $\Sigma N$  effective interaction may be approximately simulated by replacing  $V$  by  $\tilde{V}$ :

$$\tilde{V}(r) = (t\sqrt{\pi})^{-3} \int d\mathbf{r}' V(r') \exp(-(\mathbf{r} - \mathbf{r}')^2 t^2), \quad (9)$$

with  $t \simeq 1$  fm.

As an example let us consider the lower level in the  $\Sigma^-$ -Pb atom. When in our calculation we replace  $V$  by  $\tilde{V}$ , we obtain for the energy shift and width:  $\tilde{\epsilon} = 510$  eV and  $\tilde{\Gamma} = 738.4$  eV. A comparison with the results in table 1 shows that the finite range of the effective  $\Sigma N$  interaction represented by eq. (9) changes  $\epsilon$  by  $(\tilde{\epsilon} - \epsilon)/\epsilon = \Delta\epsilon/\epsilon = 11.7\%$  and  $\Gamma$  by  $(\tilde{\Gamma} - \Gamma)/\Gamma = \Delta\Gamma/\Gamma = -4.5\%$ . The finite-range corrections of this magnitude would certainly not change the conclusions based on our LDA results.

In calculating the absorptive potential  $W$ , we apply parametrization (8) for the total  $\Sigma A$  conversion cross-section  $\sigma$ . However, the experimental points to which parametrization (8) is adjusted have big error bars. Furthermore, we need in expression (5) for  $W_{MN}$  the cross-section  $\sigma$  at the average  $\Sigma^-$  momentum  $\bar{p}_\Sigma = \hbar\bar{k}_\Sigma$  which varies from 13 MeV/ $c$  for the upper level in  $^{12}\text{C}$  to 80 MeV/ $c$  for the lower level in  $^{208}\text{Pb}$ . Now, the experimental points start at 110 MeV/ $c$ , and thus we use parametrization (8) to extrapolate the values of  $\sigma$  to  $\Sigma^-$  momenta smaller than 110 MeV/ $c$ . This leads to a considerable uncertainty in  $\sigma$  and consequently in our  $W$  (which affects predominantly our results for  $\Gamma$ ). To resolve this uncertainty one needs more low-energy data on the conversion cross-section.

In our discussion of the properties of  $\Sigma^-$  atoms, we restricted ourselves to model F of the Nijmegen baryon-baryon interactions, because — as we indicated in sect. 1 — the remaining Nijmegen models lead to  $V$  attractive inside the nucleus and are inconsistent with the pion spectra measured in the  $(K^- \pi)$  reactions. Nevertheless, it is interesting to see which values of energy shifts and widths in  $\Sigma^-$  atoms would one obtain by applying these remaining interaction models.

As we see in fig. 1, interaction models D and NSC lead to an attractive  $\Sigma$  s.p. potential  $V$  which at all densities is more attractive than  $V_F$ , the s.p. potential in the case of model F. Consequently, we expect that in the case of models D and NSC the energy shifts  $\epsilon$  should be much bigger than in the case of model F (and thus also much bigger than the experimental shifts). Because of the stronger attraction, the  $\Sigma^-$  hyperon is pulled more into the region of stronger absorptive potential  $W$ , and we expect that in the case of models D and NSC also the widths  $\Gamma$  should be much bigger than in the case of model F (and in experiment). The situation with model SC is different — here at very low densities  $V$  is less attractive than  $V_F$ , and to see whether model NSC is consistent with the  $\Sigma^-$  atomic data, we simply have to calculate  $\epsilon$  and  $\Gamma$ .

Our results obtained for  $\epsilon$  and  $\Gamma$  in the  $\Sigma^-$ -Pb atom in the case of models D, SC, and NSC are shown in table 2 which also contains values of  $\chi^2(\text{Pb})$  calculated for the 3 experimental Pb data points (for model F, we have

**Table 2.** Energy shifts  $\epsilon$ ,  $\epsilon^u$  and widths  $\Gamma$ ,  $\Gamma^u$  calculated with the indicated models of the  $\Sigma N$  interaction, respectively for the lower and upper level of the  $\Sigma^-$ -Pb atom and the corresponding values of  $\chi^2$  for the 3 experimental Pb data (see table 1). All energies are in eV.

Model	$\epsilon$	$\Gamma$	$\epsilon^u$	$\Gamma^u$	$\chi^2(\text{Pb})$
D	995.4	1250.9	29.7	29.0	148.0
SC	380.0	877.4	12.6	24.7	15.2
NSC	1899.5	2603.8	49.3	37.7	933.2

**Table 3.** Energy shifts  $\epsilon$ ,  $\epsilon^u$  and widths  $\Gamma$ ,  $\Gamma^u$  calculated with model SC of the  $\Sigma N$  interaction, respectively for the lower and upper level of the indicated  $\Sigma^-$  atoms. All energies are in eV.

Nucleus	$\epsilon$	$\Gamma$	$\epsilon^u$	$\Gamma^u$
$^{12}\text{C}$	6.79	24.8	0.004	0.011
$^{16}\text{O}$	63.0	245.2	0.066	0.21
$^{24}\text{Mg}$	10.2	47.4	0.021	0.096
$^{27}\text{Al}$	24.4	109.4	0.064	0.27
$^{28}\text{Si}$	43.6	226.0	0.14	0.66
$^{32}\text{S}$	137.5	814.4	0.67	3.19
$^{40}\text{Ca}$	7.5	39.0	0.028	0.14
$^{48}\text{Ti}$	61.1	117.3	0.39	0.50
$^{138}\text{Ba}$	92.3	91.2	1.85	1.51
$^{184}\text{W}$	87.6	190.4	2.23	4.29
$^{208}\text{Pb}$	380.0	877.4	12.6	24.7

$\chi^2(\text{Pb})_F = 10.3$ ). Results for models D and NSC fully agree with our expectation and we see that these models are completely inconsistent with the  $\Sigma^-$  atomic data. Also for model SC we have  $\chi^2(\text{Pb})_{\text{SC}} > \chi^2(\text{Pb})_F$ , however the difference between the results obtained with models SC and F is less drastic. For this reason, in the case of model SC, we have calculated  $\epsilon$  and  $\Gamma$  for all  $\Sigma^-$  atoms considered in the case of model F, and our results are shown in table 3. For the 23 data points we obtained  $\chi_{\text{SC}}^2 = 55.0$ , whereas with model F we have a smaller value of  $\chi_F^2 = 38.1$ . Thus we conclude, that  $\Sigma^-$  atomic data alone eliminate models D and NSC, and among models F and SC clearly favor model F.

We consider as the essential conclusion of this work, that the analysis of both  $(K^-, \pi)$  and  $\Sigma^-$  atomic data shows that the potential felt by the  $\Sigma$  hyperon inside the nucleus is repulsive.

Part of this work was accomplished during the visit of one of the authors (JD) at the National Centre for Scientific Research “Democritos”, and he expresses his gratitude to G.S. Anagnostatos for his invitation and hospitality. He also is indebted to S. Wycech for several illuminating discussions, and to A. Gal and E. Friedman for sending him their Pb results. This research was partly supported by the Komitet Badań Naukowych under Grant No. 2P03B7522 and by the NATO Fellowship Programme.

## Appendix A.

The exclusion principle operator  $Q$  is a projection operator onto nucleon states above the Fermi sea in the  $\Lambda N$  channel. It acts in the final state of the  $\Sigma\Lambda$  conversion process in which  $\Sigma^-$  with momentum  $\mathbf{k}_\Sigma$  collides with nucleon (proton) with momentum  $\mathbf{k}_N$ . The collision leads to the final state:  $\Lambda$  with momentum  $\mathbf{k}'_\Lambda$  and nucleon (neutron) with momentum  $\mathbf{k}'_N$ .  $Q$  depends on the total and relative  $\Lambda N$  momenta,  $\mathbf{K}$  and  $\mathbf{k}'_{\Lambda N}$ . We approximate  $Q$  by its average over the angle between  $\mathbf{K}$  and  $\mathbf{k}'_{\Lambda N}$ :

$$\begin{aligned} Q(K, k'_{\Lambda N}) &= 1, \quad \text{for } |k'_{\Lambda N} - \mu_{\Lambda N}K/M_\Lambda| > k_F, \\ &= 0, \quad \text{for } k'_{\Lambda N} + \mu_{\Lambda N}K/M_\Lambda < k_F, \\ &= [(k'_{\Lambda N} + \mu_{\Lambda N}K/M_\Lambda)^2 - k_F^2] / (4\mu_{\Lambda N}Kk'_{\Lambda N}/M_\Lambda) \\ &\quad \text{otherwise,} \end{aligned} \quad (\text{A.1})$$

where  $\mu_{\Lambda N}$  is the  $\Lambda N$  reduced mass. Obviously, we have  $k_N < k_F$  and  $k'_N > k_F$ , where  $k_F$  is the Fermi momentum.

To determine  $k'_{\Lambda N}$ , we use the conservation of total momentum,

$$\mathbf{K} = \mathbf{k}_N + \mathbf{k}_\Sigma = \mathbf{k}'_N + \mathbf{k}'_\Lambda, \quad (\text{A.2})$$

and the energy conservation,

$$e_N(k_N) + e_\Sigma(k_\Sigma) + \Delta = e_N(k'_N) + e_\Lambda(k'_\Lambda), \quad (\text{A.3})$$

where  $e_N$ ,  $e_\Sigma$ ,  $e_\Lambda$  are s.p. energies of  $N$ ,  $\Sigma$ ,  $\Lambda$  in nuclear matter, and  $\Delta = (M_\Sigma - M_\Lambda)c^2$ .

For all the s.p. energies we assume quadratic momentum dependence, *i.e.*, the effective mass approximation:

$$e_N(k_N) = \frac{1}{\nu}[\epsilon_N(k_N) - \epsilon_N(k_F)] + e_N(k_F), \quad (\text{A.4})$$

$$e_N(k'_N) = \frac{1}{\nu'}[\epsilon_N(k'_N) - \epsilon_N(k_F)] + e_N(k_F), \quad (\text{A.5})$$

$$e_\Sigma(k_\Sigma) = \frac{1}{\nu_\Sigma}\epsilon_\Sigma(k_\Sigma) + D_\Sigma, \quad (\text{A.6})$$

$$e_\Lambda(k'_\Lambda) = \frac{1}{\nu_\Lambda}\epsilon_\Lambda(k'_\Lambda) + D_\Lambda, \quad (\text{A.7})$$

where  $\epsilon_X$  denotes the  $X$  kinetic energy ( $X = N, \Sigma, \Lambda$ ).

We identify  $e_N(k_F)$  with the nucleon separation energy  $\partial E_{\text{NM}}/\partial A$ :

$$\begin{aligned} e_N(k_F) &= \partial E_{\text{NM}}/\partial A = E_{\text{NM}}/A + \frac{1}{3}d(E_{\text{NM}}/A)/dk_F = \\ &= \epsilon_N(k_F) + 2bk_F^3 + \frac{7}{3}ck_F^4, \end{aligned} \quad (\text{A.8})$$

where in the last step we assumed the energy of nuclear matter per nucleon in the form

$$E_{\text{NM}}/A \equiv f(k_F) = \frac{3}{5}\epsilon_N(k_F) + bk_F^3 + ck_F^4. \quad (\text{A.9})$$

The requirement that nuclear matter saturates at  $k_F = k_{F0} = 1.35 \text{ fm}^{-1}$  with  $f(k_{F0}) = -15.8 \text{ MeV}$  fixes the values of  $b = -44.1 \text{ MeV fm}^3$  and  $c = 21.1 \text{ MeV fm}^4$  (they lead to a reasonable value of the compressibility,  $k_{F0}^2 [d^2 f/dk_F^2]_0 = 240 \text{ MeV}$ ).

With expression (A.8) for  $e_N(k_F)$ , eq. (A.4) takes the form

$$e_N(k_N) = \frac{1}{\nu}\epsilon_N(k_N) + [1 - \frac{1}{\nu}]\epsilon_N(k_F) + 2bk_F^3 + \frac{7}{3}ck_F^4, \quad (\text{A.10})$$

and eq. A.5) for  $e_N(k'_N)$  takes the same form except that  $\nu$  has to be replaced by  $\nu'$ , and  $k_N$  by  $k'_N$ .

To determine  $\nu$  we assume that our s.p. energy  $e_N(k_N)$  leads to the correct energy per nucleon  $E_{\text{NM}}/A$ :

$$\frac{1}{2}\langle \epsilon_N + e_N \rangle = f(k_F), \quad (\text{A.11})$$

and obtain

$$1/\nu = 1 + \frac{5}{6}ck_F^4/\epsilon_N(k_F). \quad (\text{A.12})$$

For the dependence of  $\nu'$  on  $\rho$ , we use the form [32]

$$1/\nu' = 1 + (1/\nu'_0 - 1)\rho/\rho_0, \quad (\text{A.13})$$

where  $\nu'_0$  is the value of  $\nu'$  at the equilibrium density  $\rho_0$ . We use the value  $\nu'_0 = 0.7$  compatible with the empirical energy dependence of the real part of the nuclear optical potential [33].

For the hyperon effective mass parameters,  $\nu_Y$  ( $Y = \Sigma, \Lambda$ ), we use expression (A.13) with  $\nu'$  replaced by  $\nu_Y$  and  $\nu'_0$  by  $\nu_{Y0} = \nu_Y|_{\rho=\rho_0}$ . Values of  $\nu_Y$  are not well known. We assume that  $\nu_\Lambda \equiv \nu'$ , which is supported by early estimates [34] and which simplifies the resulting expression for  $k'_{\Lambda N}$ . In our calculations, we assume that also  $\nu_\Sigma \equiv \nu'$ .

$D_\Sigma$  in eq. (A.6) is identical with  $V_0(k_\Sigma = 0, \rho)$  which—calculated with the YNG interaction—is shown in fig. 1. In the same way—with the help of the YNG interaction—we have calculated  $D_\Lambda$ .

With the above results for all the s.p. energies, our final expression for  $k'_{\Lambda N}$ , which follows from the total momentum and energy conservation, is

$$\begin{aligned} \frac{\hbar^2 k'^2_{\Lambda N}}{2\mu_{\Lambda N}\nu'} &= \frac{\hbar^2 k^2_{\Sigma N}}{2\mu_{\Sigma N}\nu} + \frac{1}{2}\hbar^2 K^2 \\ &\times \left[ \frac{1}{(M_N + M_\Sigma)\nu} - \frac{1}{(M_N + M_\Lambda)\nu'} \right] \\ &+ \left( \frac{1}{\nu_\Sigma} - \frac{1}{\nu} \right) \epsilon_\Sigma(k_\Sigma) + \left( \frac{1}{\nu'} - \frac{1}{\nu} \right) \epsilon_N(k_F) \\ &+ D_\Sigma - D_\Lambda + \Delta. \end{aligned} \quad (\text{A.14})$$

With  $k'_{\Lambda N}$  determined from eq. (A.14), we have calculated  $Q$ , eq. (A.1). With this  $Q$  and with  $\nu'$  determined from eq. (A.13), we have calculated  $W_{\text{NM}}$ , eq. (5), and  $W(r)$ , eq. (6). This procedure is important inside nuclei, where  $\rho \simeq \rho_0$ . At lower densities  $\rho$ , relevant in  $\Sigma^-$  atoms, we have approximately  $Q \simeq 1$  and  $\nu' \simeq 1$ , and a much simpler procedure, applied in [29], appears justified.

## References

1. C.J. Batty, E. Friedman, A. Gal, Phys. Rep. **287**, 385 (1997).
2. R.J. Powers *et al.*, Phys. Rev. C **47**, 1263 (1993).
3. J. Dąbrowski, J. Rożynek, Acta Phys. Pol. B **29**, 2147 (1998).
4. Y. Shimizu, Ph.D. thesis, University of Tokyo (1996) unpublished.
5. J. Dąbrowski, Phys. Rev. C **60**, 025205 (1999).
6. R. Sawafta, Nucl. Phys. A **585**, 103c (1995); S. Bart *et al.*, Phys. Rev. Lett. **83**, 5238 (1999).

7. R. Bertini *et al.*, Phys. Lett. B **90**, 375 (1980); **158**, 19 (1985).
8. T. Nagae *et al.*, Phys. Rev. Lett. **80**, 1605 (1998).
9. T. Harada, Phys. Rev. Lett. **81**, 5287 (1998).
10. J. Mareš, E. Friedman, A. Gal, B.K. Jennings, Nucl. Phys. A **594**, 311 (1995).
11. N.M. Nagels, T.A. Rijken, J.J. de Swart, Phys. Rev. D **12**, 744 (1975); **15**, 2547 (1977).
12. N.M. Nagels, T.A. Rijken, J.J. de Swart, Phys. Rev. D **20**, 1663 (1979).
13. P.M.M. Maessen, T.A. Rijken, J.J. de Swart, Phys. Rev. C **40**, 2226 (1989); Nucl. Phys. A **547**, 245c (1992).
14. T.A. Rijken, V.G. J. Stoks, Y. Yamamoto, Phys. Rev. C **59**, 21 (1999).
15. Y. Yamamoto, T. Motoba, H. Himeno, K. Ikeda, S. Nagata, Progr. Theor. Phys. Suppl. **117**, 361 (1994).
16. J. Dąbrowski, Acta Phys. Pol. B **30**, 2783 (1999).
17. T. Yamada, Y. Yamamoto, Progr. Theor. Phys. Suppl. **117**, 241 (1994).
18. J. Dąbrowski, J. Rozynek, Acta Phys. Pol. B **14** 439 (1983).
19. J. Dąbrowski, J. Rozynek, Phys. Rev. C **23**, 1706 (1981).
20. A. Gal, C.B. Dover, Phys. Rev. Lett. **44**, 379 (1980).
21. A. Gal, G. Toker, Y. Alexander, Ann. Phys. (N.Y.) **137**, 341 (1981).
22. G.S. Anagnostatos, Can. J. Phys. **70**, 361 (1992).
23. G.S. Anagnostatos, Int. J. Theor. Phys. **24**, 579 (1985).
24. G.S. Anagnostatos, P. Ginis, J. Giapitzakis, Phys. Rev. C **58**, 3305 (1998).
25. C.W. De Jager, H. De Vries, C. De Vries, At. Data Nucl. Data Tables **14**, 479 (1974).
26. G.S. Anagnostatos, Int. J. Mod. Phys. E **5**, 557 (1996).
27. G. Backenstoss, T. Bunacin, J. Egger, H. Koch, A. Schwit-ter, L. Tauscher, Z. Phys. A **273**, 137 (1975).
28. C.J. Batty, S.F. Biagi, M. Blecher, S.D. Hoath, R.A.J. Rid-dle, B.L. Roberts, J.D. Davies, G.J. Pyle, G.T.A. Squier, D.M. Asbury, Phys. Lett. B **74**, 27 (1978).
29. J. Dąbrowski, J. Rozynek, G.S. Anagnostatos, Acta Phys. Pol. B **32**, 2179 (2001).
30. J. Rozynek, J. Dąbrowski, Phys. Rev. C **20**, 1612 (1979).
31. J.P. Jeukenne, A. Lejeune, C. Mahaux, Phys. Rev. C **16**, 80 (1977).
32. B. Friedman, V.R. Pandharipande, Phys. Lett. B **100**, 205 (1981).
33. A. Bohr, B. Mottelson, *Nuclear Structure*, Vol. I (W.A. Benjamin Inc., 1969) p. 237.
34. H. Bandō, S. Nagata, Progr. Theor. Phys. **67**, 522 (1982); Y. Yamamoto, H. Bandō, Progr. Theor. Phys. Suppl. **81**, 9 (1985); K.F. Chong, Y. Nogami, E. Satoh, Can. J. Phys. **48**, 2804 (1970).